



Master on
Key Enabling
Technologies
4 Food and
+ Bioprocess

UNIVERSITAT POLITÈCNICA DE CATALUNYA
ESCUELA SUPERIOR D'AGRICULTURA DE BARCELONA
MASTER'S DEGREE IN ENABLING TECHNOLOGIES FOR THE FOOD AND
BIOPROCESSING INDUSTRY

**Use of consumer-grade cameras to assess barley
and wheat N status and grain yield**

Presented by :

Karima Figuigui

Supervised by :

Lydia Serrano Porta and Gil Gorchs Altarriba

Department of Agri-Food Engineering and Biotechnology

Universitat Politècnica de Catalunya

ACKNOWLEDGEMENTS

First of all, I would like to thank God all his blessings especially patience and perseverance to keep pursuing my educational journey and continue to challenge myself to prepare more and achieve more.

Secondly, I would like to express my genuine gratitude towards the following inspiring individuals who their presence was critical for my success :

Thanks to the program coordinators Montserrat Casas Carbonell and Nuria Carazo Gómez for having authorized me to enroll in this master.

A profound Thanks to my tutor Lydia Serrano Porta for allowing me to carry out my internship with her, for her supervision, her confidence in me, and her support during these previous 5 months.

A deep appreciation towards my co-tutor Gil Gorchs Altarriba for his help, confidence, and support to join the project.

Thanks to all Professors of KET4FOOD Master for their efforts, presence, kindness, and permanent support especially during the quarantine and this tough pandemic period.

A profound thanks to all the members of the jury, who have honored me by agreeing to judge my modest work, and to everyone who contributed either directly or indirectly in the progress of this report.

Finally, I would like to show my pure gratitude to my family and friends for their existence, their continuous support to my decisions, their belief in me, and offering me the needed help to achieve my goals.

LIST OF ABBREVIATIONS

ANOVA: Analysis of Variance

B/R: Blue Red Simple Ratio

CCI: Chlorophyll Content Index

CCM: Chlorophyll Content Meter

fIPAR: fractional Intercepted Photosynthetic Active Radiation

GIS: Geographical Information Systems

GNDVI: Green Normalized Vegetation Index

GPS: Global Positioning Systems

GY: Grain Yield

N: Nitrogen

NDVI: Normalized Difference Vegetation Index

NIR: Near Infra-Red

NUE: Nitrogen Use Efficiency

GPC: Grain Protein content

R_{xx}: Reflectance

R: Red

SNK: Student-Newman-Keuls

VARI: Visible Atmospherically Resistant Index

VI: Vegetation Indices

TABLE OF CONTENTS

1. Introduction.....	1
2. Objectives.....	7
3. Materials and methods.....	8
3.1. Experimental site and crop management	8
3.2. Field data collection.....	8
3.3. Statistical analyses	10
4. Results	12
4.1. <i>Hordeum vulgare</i> L	12
4.1.1. <i>Optical indices (fIPAR and CCI) values</i>	12
4.1.2. <i>Relationships among crop data (biomass, and grain yield and grain protein content) and canopy biophysical attributes (fIPAR and CCI)</i>	12
4.1.3. <i>Relations between the fIPAR and CCI and spectral data (vegetation indices and color coordinates)</i>	13
4.1.4. <i>The capability of spectral indices at distinguishing crop N status and their effects on grain yield and protein content</i>	17
4.2. <i>Triticum aestivum</i> L.....	19
4.2. 1. <i>Optical indices (fIPAR and CCI) values</i>	19
4.2. 2. <i>Relationships among crop data (biomass, and grain yield and grain protein content) and canopy biophysical attributes (fIPAR and CCI)</i>	19
4.2. 3. <i>Relationships between the fIPAR and CCI and spectral data (vegetation indices and color coordinates)</i>	20
4.2. 4. <i>The capability of spectral indices at distinguishing crop N status and their effects on grain yield and protein content.</i>	23
5. Discussion	25
6. CONCLUSIONS AND FUTURE LINES.....	28

INDEX OF TABLES

Table I: The several Color space used in images' processing in this study	9
Table II: Vegetation indices derived from red (R), green (G), blue (B), and near-infrared (NIR) bands acquired with a consumer-grade camera used in this study.....	11
Table III: Correlation coefficients between the fraction of intercepted PAR (fIPAR), the chlorophyll content index (CCI), biomass, yield, and protein content at the anthesis stage for barley (n = 12).....	13
Table IV: Correlation coefficients between the fraction of intercepted PAR (fIPAR), the chlorophyll content index (CCI), and the vegetation indices (VI) obtained with a modified conventional digital camera for barley (n = 12).....	14
Table V: Barley correlation coefficients between biomass, yield, and protein content and vegetation indices obtained with a modified conventional digital camera (n = 12).	15
Table VI: The Pearson correlation values between the fIPAR and CCI and the parameters of different color coordinates.	16
Table VII: Correlation coefficients between the fraction of intercepted PAR (fIPAR), the chlorophyll content index (CCI), biomass yield, grain yield, and protein content for wheat at anthesis phenological stage (n = 12).	20
Table VIII: Correlation coefficients between the fraction of intercepted PAR (fIPAR), the chlorophyll content index (CCI), and the vegetation indexes (VI) obtained for wheat with a modified conventional digital camera (n = 12).	20
Table IX: Correlation coefficients between biomass, yield, and protein content and vegetation indices (VI) obtained for wheat with a modified conventional digital camera (n = 12).	22
Table X: The Pearson correlation values between the fIPAR and CCI and the parameters of different color coordinates of wheat.....	22

INDEX OF FIGURES

Figure 1: Nitrogen as a key component of biomass (left) and its proportional allocation in a C3 plant leaf (right).....	2
Figure 2: Optimal periods for nitrogen fertilization application (Scharf & Grundler, n.d.).....	3
Figure 3 : (A) Fractional Intercepted Photosynthetic Active Radiation (fIPAR) and (B) leaf Chlorophyll Content Index (CCI) at the anthesis phenological stage for barley. Data are average values for each treatment and bars represent the standard error of the mean (n = 3).	12
Figure 4: Relationships derived from the conventional camera between the BR vegetation index with fIPAR (a), between BR and CCI (b), and between the VARI vegetation index with CCI (c) for barley (n = 12).	15
Figure 5 : (A) Fractional Intercepted Photosynthetic Active Radiation (fIPAR), (B) leaf Chlorophyll Content Index (CCI), (C) Protein content (PC), (D) grain yield (GY),(E) Blue Red Simple Ratio (BR) and (F) Visible Atmospherically Resistant Index (VARI) at anthesis phenological stage for barley. Data are average values for each treatment and bars represent the standard error of the mean (n = 3).....	18
Figure 6 : (A) Fractional Intercepted Photosynthetic Active Radiation (fIPAR) and (B) leaf Chlorophyll Content Index (CCI) at the anthesis phenological stage for wheat. Data are average values for each treatment and bars represent the standard error of the mean (n = 3).	19
Figure 7: Correlations between the different vegetation indices of wheat and fIPAR and CCI: between the NDVI and GNDVI indices and fIPAR (a) and (b), and between VARI and CCI (c) (n = 12).....	21
Figure 8 : (A) Fractional Intercepted Photosynthetic Active Radiation (fIPAR), (B) leaf Chlorophyll Content Index (CCI), (C) grain yield (GY), (D) Protein content (PC), (E) Normalized Difference Vegetation Index (NDVI) and (F) Green Normalized Vegetation Index (GNDVI)at anthesis phenological stage for wheat according to SNK. Data are average values for each treatment and bars represent the standard error of the mean (n = 3).	24

Abstract

In rain-fed crops, nitrogen (N) is a key factor determining cereal productivity and grain quality. Assessment of the cereal N status permits to optimize N fertilizer input and reduce environmental impacts while improving N-use efficiency and both grain yield (GY) and protein content (GPC). Consumer-grade digital cameras are recognized as a cost-effective remote sensing technique of monitoring plant N status. To explore the feasibility of using consumer-grade cameras to diagnose the N status and to predict grain yield, biomass, and protein content (GPC), a field experiment was conducted in *Hordeum vulgare* L and *Triticum aestivum* L at different N rates (0, 60, 120 and 180 kg.N.ha⁻¹). Measurements were carried at the anthesis stage to determine biomass, grain yield, and protein content at harvest. The capacity of vegetation indices formulated using blue (B), green (G), red (R), and near-infrared (NIR) bands obtained with a consumer-grade camera to assess N status was evaluated. The results showed a high correlation between multiple vegetation indices and canopy biophysical attributes CCI and fIPAR (Chlorophyll Content Index and fractional Intercepted and Photosynthetic Active Radiation); The indices VARI and BR presented the higher correlation with CCI for barley with $P < 0,01$ and $r = 0,786$, $r = 0,800$ successively, and BR was the only index which correlates with fIPAR with $r = 0,583$ and $P < 0,05$. Whereas for wheat, all indices were highly correlated with CCI and fIPAR, and the indices which relate the NIR band to the R (NDVI) and G (GNDVI) bands in addition to the index that relates blue to red bands presented the best correlations in all parameters ($r > 0,800$ and $P < 0,01$). Moreover, the indices BR, VARI, and NDVI_{rgb} permitted the estimation of GPC in both species, and in the estimation of biomass and grain yield, the correlations obtained through the modified conventional were high and significant. Consequently, consumer-grade cameras based on vegetation indices may have great potential for grain yield prediction and crop N status assessment.

Keywords: *Hordeum vulgare* L, *Triticum aestivum* L, N status, grain protein content, consumer-grade cameras, remote sensing

1. Introduction

Barley (*Hordeum vulgare* L.) is a cereal belonging to the family *Poaceae*, the tribe *Triticeae*, and the genus *Hordeum*. It is the fourth most important cereal crop in the world after wheat, corn, and rice (Vasanthan & Hoover, 2009). Barley and wheat (*Triticum aestivum* L.), which is the third most important crop in terms of global production, have been important crops for thousands of years and continues to be widely used for human nutrition, animal feed, malting, and brewing in the present day (Wilkinson, 2019). Application of proper nutrients is necessary to get a high yield from a crop and generally nitrogen (N) is considered to be the most important factor for determining productivity and grain quality in the current cropping systems employed around the world (Ma et al., 2019). Nitrogen (N) availability is essential for obtaining high yield potential, as it influences the numbers of tillers emitted and those surviving, the number of grains per spike, the grain weight, and protein content (Mantai et al., 2016; Vian et al., 2018). The protein content of wheat is largely influenced by several factors including available N. If N supply remains constant, increased yield usually results in a decrease in protein content due to dilution of N by the larger biomass (Gauer et al., 1992). Plant growth dominantly depends on the N supply. A deficiency in N would reduce crop photosynthesis, whereas higher rates of N fertilization do not necessarily improve crop yield and can lead to serious groundwater pollution (Jiang et al., 2019; Mulla, 2013; Vitousek et al., 2009).

Nitrogen deficiency negatively affects photosynthetic assimilation and crop yield both in terms of quantity and quality. Therefore, fertilizer application rates for optimal economic and environmental yield should be considered by taking into account the individual needs of genotypes as well as their actual uptake rates depending on growth stage, soil, and weather conditions (Berger et al., 2020; Jay et al., 2017).

The functions of N are structural and osmotic. The structural ones are specific and are related to the synthesis of molecules essential for growth, such as nucleic acids, amino acids, proteins, chlorophylls, and alkaloids. The osmotic function is associated with the effect of nitrate ion and other reduced forms of N, in the reduction of the water potential (Ψ_w) of the vacuole, within the osmoregulation process. Considering that water is the main limiting factor in plant development and that it is the only substance capable of integrating growth and metabolic activity at the cellular level, the function of N as an osmotic agent, which allows water to be

retained in vacuoles, has been considered as important than its nutritional function (Cárdenas-Navarro et al., 2004).

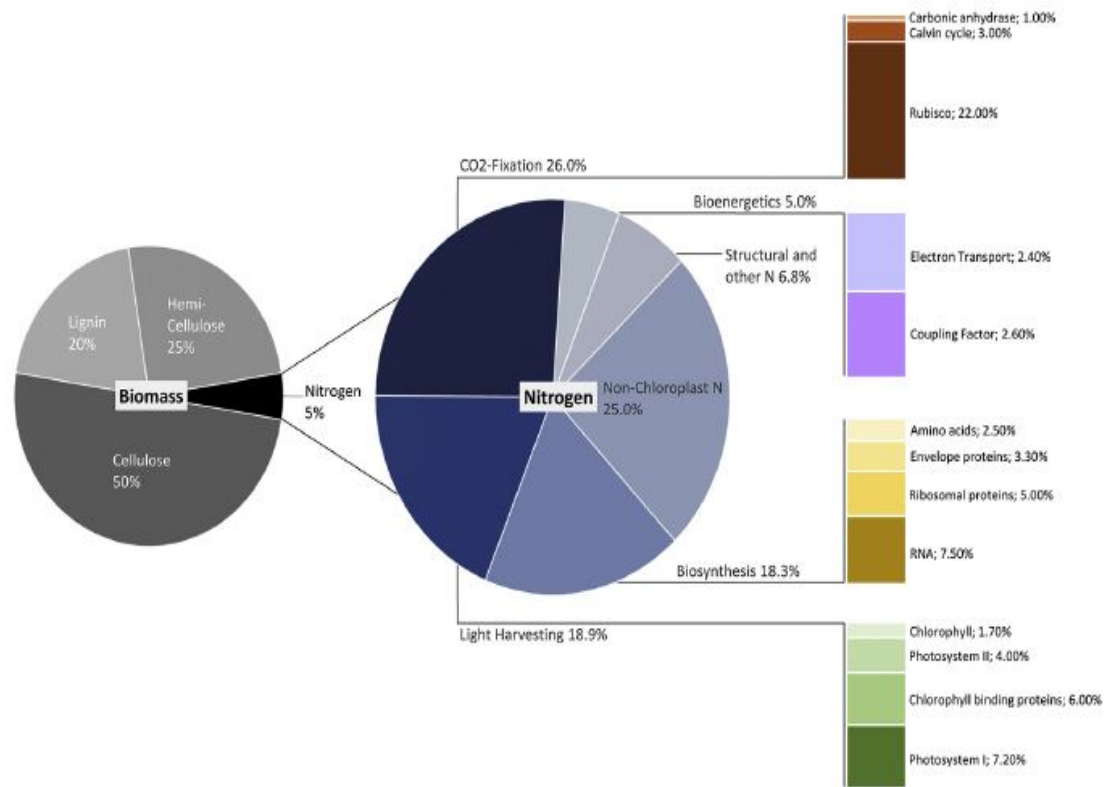


Figure 1: Nitrogen as a key component of biomass (left) and its proportional allocation in a C3 plant leaf (right) (Berger et al., 2020).

Excessive or improper nitrogen (N) application rates negatively affect crop production and thereby environmental quality. Therefore, it is very important to optimize N fertilizer input to balance grain yield, environmental risk, and benefits. Excessive N application does not significantly improve crop yields, and it can decrease N use efficiency (NUE) and also cause serious environmental problems due to the loss of a large amount of applied N into the environment (Ma et al., 2019; Vitousek et al., 2009).

In all crops, rapid uptake of N occurs during the maximum growth period. There is not much risk of N loss when fertilizer is applied at the beginning of the period of rapid growth (Scharf & Grundler, n.d.). N application after the booting has been shown to increase grain protein content (Nakano et al., 2008). In Ireland, the currently recommended timing for the first application of fertilizer N to winter wheat is between late tillering and the onset of stem elongation. In practice, many growers apply N in late February/early March, often in advance of significant spring growth, which may be leading to reduced nitrogen use efficiency (NUE) (Efretuei et al., 2016). (Fischbeck & Muller, 1990) reported that excess N applications before the wheat crop began stem extension, particularly in areas where there was high N supply from the soil, could lead to reductions in yield. The application of N fertilizer can increase both yield and protein content. If the wheat yield is limited due to N deficiency, small additions of N will increase crop yield without significantly increasing protein. The protein content is increased by N application above the point where N is no longer the factor most limiting to yield. The lag phase in protein response to N application increases as growth conditions and/or yield potential of the cultivar improve since a greater amount of N is required for production when yield potential is higher. Changes in protein content with the application of fertilizer N differ with cultivar (Gauer et al., 1992).

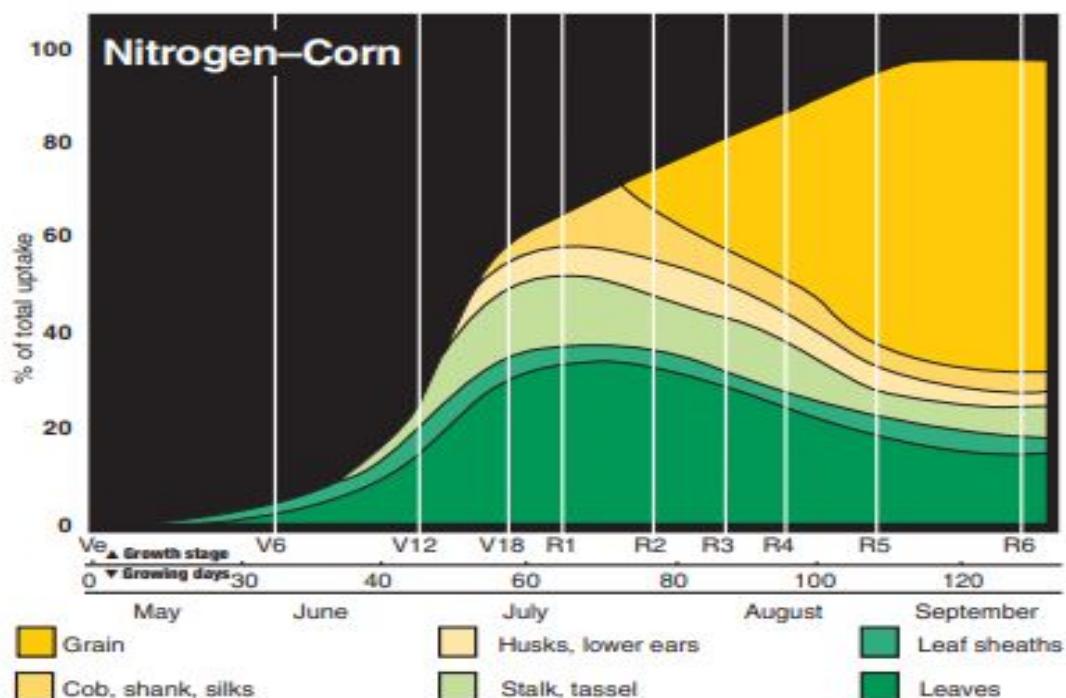


Figure 2: Optimal periods for nitrogen fertilization application (Scharf & Grundler, n.d.)

Maximum nitrogen uptake occurs in periods of maximum growth (in corn roughly between vegetative growth stages V9 and V18, or from hip-high to just before tasseling). The risk of N loss is low during this period (Scharf & Grundler, n.d.).

In some mainly developed countries, new technology is emerging applied to the management of agricultural production systems. This technology, called Precision Agriculture, involves intensive mapping of soil characteristics and crop monitoring with computerized data management methods, Global Positioning Systems (GPS), Geographical Information Systems (GIS), and Remote Sensing (RS) for the determination of planting densities, as well as the amounts and frequency of application of pesticides and fertilizers (Cárdenas-Navarro et al., 2004). Key components of precision agriculture are (i) identifying the site-specific factors that influence within-field crop yield variation and (ii) spatially characterizing those factors (Corwin et al., 2004).

Precision agriculture has always been the research hotspot around the world. And the optimization of nitrogen fertilization for crops is the core concern. It is not only to improve the productivity of crops but also to avoid the environmental risks caused by overfertilization. Therefore, an accurate estimation of N status is crucial for determining an N recommendation. Remote sensing techniques have been widely used to monitor crops for years, and they could offer estimations for stress status diagnosis through obtaining vertical structure parameters and spectral reflectance properties of crops (Yang et al., 2014).

The use of remote sensing data solely is not sufficient to assess the actual N need since plant nitrogen and water requirements are secondary variables. It is necessary to have supplementary information to describe the crop system and this is generally achieved in two ways: either by using statistical approaches or by assimilating remote sensing data into land surface models (e.g. crop functioning, SVAT). In the operational context, data assimilation systems are still not used due to their low flexibility and complexity. Therefore, most of the systems rely on simple relationships between indices and the variable of interest (Weiss et al., 2020).

Information on vegetation development from satellite images commonly relies on indices which compare the reflectance of vegetation in multiple spectral regions. The most common indices use the differential response of vegetation in near-infrared (NIR) and red (R) or other visible bands. The normalized difference vegetation index (NDVI) is the most commonly used

(Liang et al., 2011; Nijland et al., 2014; Soudani et al., 2012). However, satellite imagery is often not the best option because of the low spatial resolution of images acquired and the restrictions of the temporal resolutions as satellites are not always available to capture the necessary images. Besides, it is often required to wait long periods between the acquisition and reception of images (Tsouros et al., 2019). As a result, the use of consumer-grade cameras to assess crop N status and monitor crops seems the best in terms of offering great possibilities to acquire field data in an easy, fast and cost-effective way

The normalized difference vegetation index is computed as the normalized differences between NIR and red reflectance [$NDVI = (R_{NIR} - R_{red}) / (R_{NIR} + R_{red})$], where R_{NIR} and R_{red} are the reflectances measured in the NIR and the red region, respectively. NDVI value varies with the absorption of red light by plant chlorophyll and the reflection of NIR radiation by water-filled leaf cells (Cabrera-Bosquet et al., 2011; Chen & Brutsaert, 1998). NDVI is considered as the most studied index for many reasons including its positive correlation with intercepted photosynthetically active radiation and also correlates well with N content. It allows assessing grain yield in field canopies and N status assessment of wheat (Cabrera-Bosquet et al., 2011; Fernández et al., 2019; Li et al., 2008).

The red-edge region is defined as the spectral region between 680 and 750 nm where there is a sharp change in the vegetation reflectance. This occurs due to the transition from chlorophyll absorption in the red region to cellular scattering in the NIR. The promise and potential of the red-edge spectral region for vegetation biophysical variable retrieval has motivated the design and also the launch of spaceborne imaging sensors involving red-edge bands, including hyperspectral satellites (Xie et al., 2018).

Remote sensing with consumer-grade cameras has been largely used in the last decade thanks to their low cost and ease of use and system deployment over multispectral cameras and scientific-grade platforms (Fernández et al., 2019).

To date, consumer-grade digital cameras comprise three major RGB bands and the full spectrum can range from 200 to 1,200 nm. The RGB ratio in each spectrum/corresponding wavelength and color is also different. A particular wavelength can be obtained using specific external or internal filters. Unlike a spectrometer, satellites, and multispectral cameras, only broadband VIs can be achieved using consumer-grade cameras. Nevertheless, previous studies have claimed that the information obtained using consumer-grade cameras is comparable to

that obtained from scientific equipment and other alternative devices, such as spectrometer and hyperspectral cameras (Putra et al., 2020).

As mentioned above, the use of images with visible and NIR bands is very common in remote sensing, especially for vegetation monitoring. Many vegetation indices such as the normalized difference vegetation index (NDVI) require spectral information in the NIR and red bands, even though the three visible bands could be sufficient for some applications. Since most consumer-grade cameras only provide the three broad visible bands, NIR filtering techniques can be used to convert a color camera to a NIR camera. Most digital cameras are fitted with filters to block UV and infrared light. Therefore, it is possible to replace the blocking filter by a long-pass infrared filter on standard CCD or CMOS sensors for obtaining NIR images. Studies have been conducted on the use of NIR-converted digital cameras for monitoring plant conditions and results from these studies support their use as simple and affordable tools for plant stress detection and growth monitoring (Yang et al., 2014).

2. Objectives

The general objective of this work is to study the potential of standard and modified consumer-grade cameras at assessing canopy traits related to crop N status, Grain Yield, and Protein Content in Barley (*Hordeum vulgare* L.) and Wheat (*Triticum aestivum* L.) under Mediterranean conditions.

The specific objectives are however multiple :

1. To study the relationships among crop variables (biomass, grain yield, and grain protein content) and canopy biophysical attributes (fIPAR and CCI)
2. To assess the relationships among spectral data (vegetation indices and color coordinates) derived from a standard and modified consumer-grade camera and optical estimates of leaf chlorophyll content (CCI) and fractional Intercepted Photosynthetic Active Radiation (fIPAR)
3. To assess the capacity of the spectral data (vegetation indices and color coordinates) derived from a standard and modified consumer-grade camera to determine grain yield and protein content
4. To compare the capability of optical and spectral data at detecting differences in crop N status and their effects on grain yield and protein content.

3. Materials and methods

3.1. Experimental site and crop management

The study was carried out in a Mediterranean climate in the experimental fields of the Escola Superior de Agricultura de Barcelona (Universitat Politècnica de Catalunya) (41°16'N 1°59'E, 4,2 m a.s.l.).

Barley (cv. Gustav) and wheat (cv. Odiel) were sown at the end of the winter (2 March 2017) in 0,15cm wide rows at a sowing density of 425 and 375 seeds per m², respectively. The experiment was organized into two randomized complete block design (wheat and barley) with Four N treatments (0 to 180 kg.N.ha⁻¹) and three replications. A plot was 10 by 1,2 m with 2 m of the border between plots which either were sown with wheat and barley, correspondingly.

3.2. Field data collection

Field measurements were made during the phenological stage of anthesis (Zadoks code 65).

Fractional intercepted PAR was determined by measuring incident PAR above the canopy (PAR_{above}) and below the canopy (PAR_{below}) at five locations per plot with an AccuPAR Ceptometer (Decagon Devices, Pullman, Washington, USA) and calculated as :

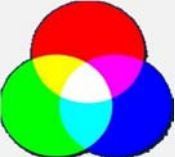
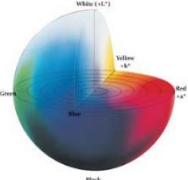
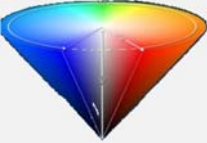
$$fIPAR = (PAR_{above} - PAR_{below}) / PAR_{above}$$

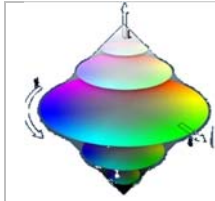
A CCM-200 leaf chlorophyll meter (Opti-Sciences, Hudson, New Hampshire, USA) was used to monitor crop N status. The CCM-200 has a 0.71-cm² measurement area and calculates a chlorophyll content index (CCI) based on absorbance measurements at two wavelengths: 653 and 931 nm. The instrument processes the proportion of light transmitted at the two wavelengths and the proportion determined in the absence of a sample to produce a digital reading (Chlorophyll Content Index, CCI) which's highly correlated with the leaf chlorophyll content (Richardson et al., 2002). Measurements were taken at the leaf longitudinal center, on the upper side, and avoiding midribs. Eight chlorophyll-meter values (chlorophyll content index, CCI) were measured on the top-most fully expanded leaves and averaged for each plot. During this study, a modified Sony NEX-5N camera has been used. The VIS, NIR, and RED filters were used while taking the images of each plot, and the images obtained are in RAW form. These images are subsequently converted to the TIFF form using Fiji software to preserve a large part of the information (pixels) and to be able to analyze them. During the use of the Fiji software, the color space used as RGB (red, blue, green) and the extension 'color transformer

2' allowed the transformation of processed images into color coordinates to see the possibility of their use as spectral indices. The color spaces used in this study are the following: RGB, HSB/HSV, Lab, HSL (Table I).

Table I: The several Color space used in images' processing in this study

(<http://colorizer.org/>;<https://sensing.konicaminolta.asia/what-is-cie-1976-lab-color-space/>)

Color space	Definition
<p data-bbox="284 526 344 555">RGB</p> 	<p data-bbox="453 526 1394 600">The RGB (Red, Green, Blue) color model is the most known, and the most used every day. It defines a color space in terms of three components :</p> <ul style="list-style-type: none"> <li data-bbox="501 616 879 645">✓ Red, which ranges from 0-255 <li data-bbox="501 660 900 689">✓ Green, which ranges from 0-255 <li data-bbox="501 705 884 734">✓ Blue, which ranges from 0-255
<p data-bbox="288 851 339 880">Lab</p> 	<p data-bbox="453 851 1382 987">The CIE 1976 L*a*b* color space (also referred to as CIELAB) is one of the most popular color spaces for measuring object colors. It was defined by CIE in 1976 for color communication and is widely adopted today in many industries for color control and management.</p> <p data-bbox="453 1025 1358 1126">In the L*a*b* color space, L* indicates lightness, and a* and b* are chromaticity coordinates. a* and b* are color directions: +a* is the red axis, -a* is the green axis, +b* is the yellow axis, and -b* is the blue axis.</p>
<p data-bbox="256 1361 371 1391">HSB/HSV</p> 	<p data-bbox="453 1205 1374 1267">The HSB (Hue, Saturation, Brightness) color model defines a color space in terms of three constituent components:</p> <p data-bbox="453 1305 1390 1395">Hue: the color type (such as red, blue, or yellow). Ranges from 0 to 360° in most applications. (each value corresponds to one color : 0 is red, 45 is a shade of orange and 55 is a shade of yellow).</p> <p data-bbox="453 1435 1366 1585">Saturation: the intensity of the color. Ranges from 0 to 100% (0 means no color, that is a shade of grey between black and white; 100 means intense color). Also sometimes called the "purity" by analogy to the colorimetric quantities excitation purity.</p> <p data-bbox="453 1626 1362 1715">Brightness (or Value): the brightness of the color. Ranges from 0 to 100% (0 is always black; depending on the saturation, 100 may be white or a more or less saturated color).</p> <p data-bbox="453 1753 1374 1843">The HSB model is also known as HSV (Hue, Saturation, Value) model. The HSV model was created in 1978 by Alvy Ray Smith. It is a nonlinear transformation of the RGB color space. In other words, color is not defined as a simple combination</p>
<p data-bbox="288 1930 339 1960">HSL</p>	<p data-bbox="453 1930 1070 1960">The HSL color space, also called HLS or HSI, stands for:</p> <ul style="list-style-type: none"> <li data-bbox="501 1975 1082 2004">✓ Hue: the color type (such as red, blue, or yellow).



Ranges from 0 to 360° in most applications (each value corresponds to one color : 0 is red, 45 is a shade of orange and 55 is a shade of yellow).

✓ Saturation: variation of the color depending on the lightness.

Ranges from 0 to 100% (from the center of the black&white axis).

✓ Lightness (also Luminance or Luminosity or Intensity).

Ranges from 0 to 100% (from black to white).

Conditions respected while field images were taken :

- Cloudless days to control and take images ;
- Positioning the camera 50cm above the canopy focusing on the center of each plot ;
- No saturation and the best dynamic range (in terms of digital numbers for each channel) of settings manipulated ;
- While taking images, a Fixed ISO value of 100 and a shutter speed of 1/1250 are used, and the white balance model was adjusted for daylight conditions ;
- Two images are required in each plot: one in standard RGB color, and one with a modified camera fitted with a 900 nm long-pass infrared filter ;

Camera's characteristics :

- Modified full-spectrum consumer-grade digital camera Sony NEX-5N ;
- Sony NEX-5N was equipped with a CMOS (complementary metal-oxide-semiconductor) sensor which is sensitive to wavelengths between 350nm and 1100nm, including ultraviolet (UV) and NIR rays ;
- Sensor Exmor APS-C CMOS 8 bit (3 channel) ;
- 16.1 megapixels (4912 x 3264) ;
- 23.5 x 15.6 mm sensor and E16 mm F2.8 fixed lens.

3.3. Statistical analyses

The data obtained were analyzed using the SPSS 22.0 statistical package (SPSS Inc., Chicago, IL, USA). Pearson's correlation coefficients between the vegetation indices, canopy biophysical variables, and the agronomic variables were calculated using a so-called bivariable procedure.

A statistical test (ANOVA) was used to test the effect of N fertilization treatments on the studied variables and means were compared using the Student-Newman-Keuls (SNK) test.

Table II: Vegetation indices derived from red (R), green (G), blue (B), and near-infrared (NIR) bands acquired with a consumer-grade camera used in this study.

Band	Name	Acronym	Formulation	Reference
NIR/R	Normalized Difference Vegetation Index	NDVI	$\frac{NIR - R}{NIR + R}$	Rouse et al. (1974) and Tucker (1979)
	Simple Ratio	SR	$\frac{NIR}{R}$	Jordan (1969), Pearson and Miller (1972)
NIR/G	Green Normalized Vegetation Index	GNDVI	$\frac{NIR - G}{NIR + G}$	Gitelson et al. (1996)
	Green simple ratio	GSR	$\frac{NIR}{G}$	Fernández et al. (2019)
B/R	Blue Red Simple Ratio	BR	$\frac{B}{R}$	Fernández et al. (2019)
B/G	Green Blue Simple Ratio	GB	$\frac{G}{B}$	(Fernández et al. 2019)
G/R	Green Red Simple Ratio	GR	$\frac{G}{R}$	(Gamon and Surfus, 1999)
	Normalized Difference Vegetation Index-Green	NDVIg	$\frac{G - R}{G + R}$	Tucker, (1979) and Gitelson, (2002)
	Soil Adjusted Vegetation Index-Green	SAVIg	$\frac{(1 + 0.5) \times (G - R)}{(G + R) + 0.5}$	Chen, (2010)
	Optimized Soil Adjusted Vegetation Index-Green	OSAVIg	$\frac{1.5 \times (G - R)}{(G + R) + 0.16}$	Widjaja Putra and Soni (2018)
R/G/B	Visible Atmospherically Resistant Index	VARI	$\frac{G - R}{(G + R) - B}$	Gitelson et al. (2002)
	Red-Green-blue Normalized Difference Vegetation Index	NDVIrgb	$\frac{(G + B) - R}{(G + B) + R}$	Widjaja et al. (2008)
	Red-Green-Blue Simple Ratio	SRrgb	$\frac{G + B}{R}$	Fernández et al. (2019)

4. Results

4.1. *Hordeum vulgare* L

4.1.1. *Optical indices (fIPAR and CCI) values*

In Figure 3, Minor variations in fIPAR and CCI among N-treatments at the anthesis phenological stage (Zadocks 65) were observed. Average fIPAR values vary between $0,73 \pm 0,047$ to $0,87 \pm 0,047$ (average \pm Standard deviation) and CCI values range from $20,81 \pm 2,253$ to $26,94 \pm 2,253$ (average \pm Standard deviation. The differences among N treatments were not significant.

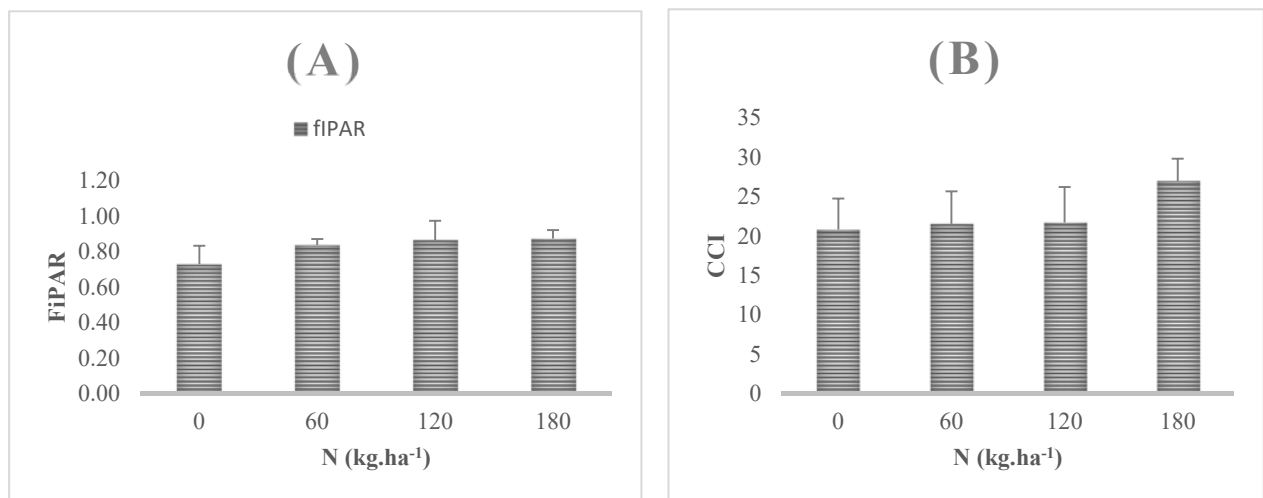


Figure 3 : (A) Fractional Intercepted Photosynthetic Active Radiation (fIPAR) and (B) leaf Chlorophyll Content Index (CCI) at the anthesis phenological stage for barley. Data are average values for each treatment and bars represent the standard error of the mean (n = 3).

4.1.2. *Relationships among crop data (biomass, and grain yield and grain protein content) and canopy biophysical attributes (fIPAR and CCI)*

The data obtained from fIPAR showed a highly significant correlation with yield parameters (Table III). On the other hand, the data obtained from the CCI showed a strong correlation with biomass yield and grain yield parameters,

Table III: Correlation coefficients between the fraction of intercepted PAR (fIPAR), the chlorophyll content index (CCI), biomass, yield, and protein content at the anthesis stage for barley (n = 12).

	Biomass avg (kg.ha ⁻¹)	Grain Yield (GY) avg (kg.ha ⁻¹)	Protein Content (PC) avg
fIPAR avg	0,300	,578*	0,543
CCI avg	,713**	,790**	0,600

* and ** indicate significant correlation at $P < 0.05$ and $P < 0.01$, respectively

4.1.3. Relations between the fIPAR and CCI and spectral data (vegetation indices and color coordinates)

The vegetation indices obtained from the combination of the visible (RGB) and infrared (NIR) bands showed a significant correlation with the biophysical variables of the canopy fIPAR and CCI (Table IV). Based on the RGB / NIR bands, the CCI correlation coefficients were slightly larger than those of fIPAR.

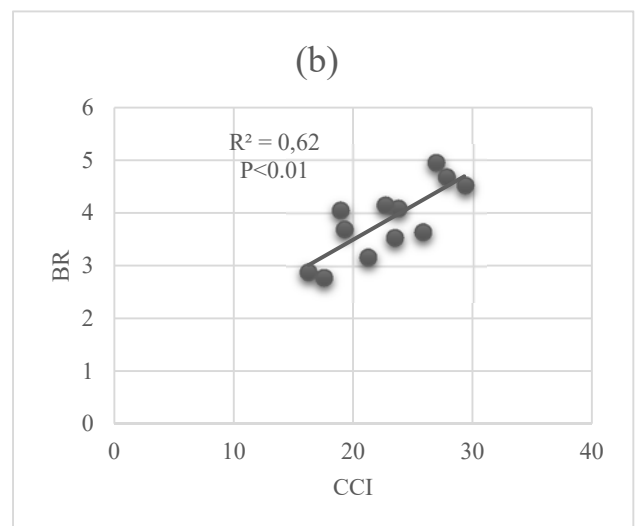
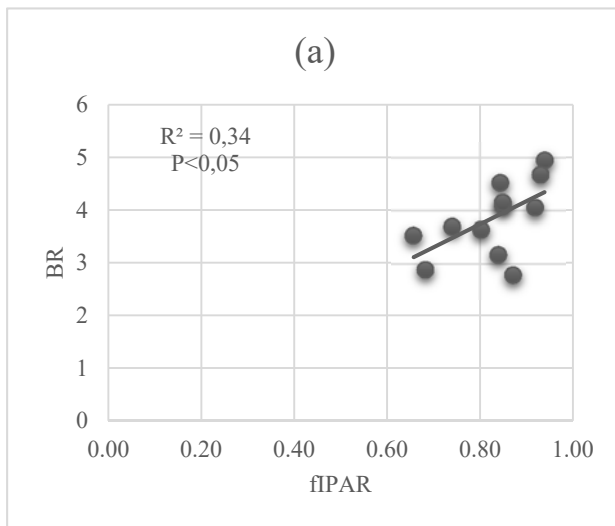
Among these indices, the visible band with the B/R ratio outperformed the other indices when estimating the fIPAR, presenting a highly significant correlation $r = 0.583$; ($P < 0.01$).

For the CCI estimation, all calculated indices presented a highly significant correlation, the index that presented the highest correlation was VARI index with $r = 0,800$ ($P < 0.01$) (in addition to BR in the same way as for fIPAR).

Table IV: Correlation coefficients between the fraction of intercepted PAR (fIPAR), the chlorophyll content index (CCI), and the vegetation indices (VI) obtained with a modified conventional digital camera for barley (n = 12).

<i>Bands</i>	<i>Relation</i>	<i>VI</i>	<i>fIPAR</i>	<i>CCI</i>
<i>NIR-VISIBLE</i>	<i>NIR/R</i>	<i>NDVI</i>	0,375	,694*
		<i>SR</i>	0,487	,703*
	<i>NIR/G</i>	<i>GNDVI</i>	0,239	,582*
		<i>GSR</i>	0,264	,595*
<i>VISIBLE</i>	<i>B/R</i>	<i>BR</i>	,583*	,786**
	<i>G/R</i>	<i>GR</i>	0,528	,719**
		<i>NDVIg</i>	0,464	,728**
		<i>VARI</i>	0,561	,800**
	<i>R/G/B</i>	<i>NDVIrgb</i>	0,488	,753**
<i>SRrgb</i>		-	-	

* and ** indicate significant correlation at $P < 0.05$ and $P < 0.01$, respectively



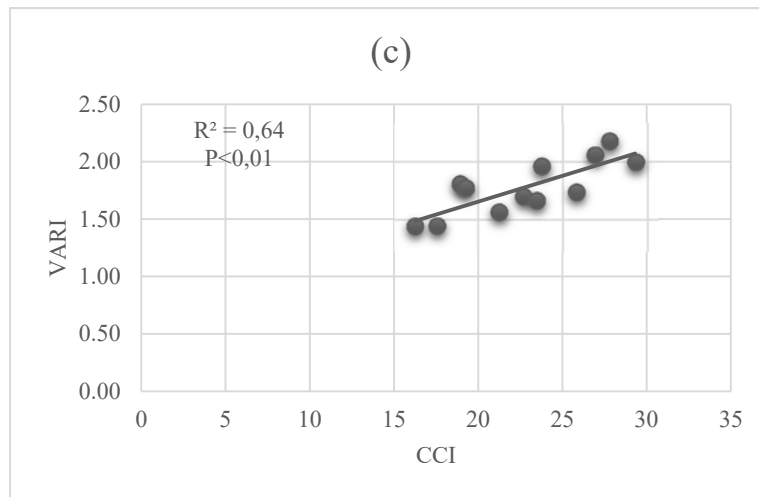


Figure 4: Relationships derived from the conventional camera between the BR vegetation index with fIPAR (a), between BR and CCI (b), and between the VARI vegetation index with CCI (c) for barley (n = 12).

The estimation of the biomass yield and grain yield, as well as grain protein content via the different plant indices grouped in Table V, showed that the two indices VARI and BR had the best correlation for the three variables simultaneously.

On the one hand, for GY, the two indices were very well correlated with values ranging from 0,770 to 0,799 ($P < 0.01$).

On the other hand, the VARI and BR indices show the best correlation with the protein content with 0,876 ($P < 0,01$) and 0.658 ($P < 0,05$) respectively.

Table V: Barley correlation coefficients between biomass, yield, and protein content and vegetation indices obtained with a modified conventional digital camera (n = 12).

	<i>VI</i>	<i>GY</i>	<i>Biomass</i>	<i>PC</i>
<i>NIR/R</i>	<i>NDVI</i>	,662*	,620*	0,519
	<i>SR</i>	,731**	,649*	0,455
<i>NIR/G</i>	<i>GNDVI</i>	,611*	,624*	0,441
	<i>GSR</i>	,623*	,625*	0,449
<i>B/R</i>	<i>BR</i>	,799**	,690*	,658*
<i>G/R</i>	<i>GR</i>	,731**	,631*	0,447
	<i>NDVIg</i>	,685*	,604*	0,516

R/G/B	VARI	,770**	,675*	,876**
	NDVI_{rgb}	,710**	,625*	0,595
	SR_{rgb}			

* and ** indicate significant correlation at $P < 0.05$ and $P < 0.01$, respectively

Table VI: The Pearson correlation values between the fIPAR and CCI and the parameters of different color coordinates.

	<i>fIPAR</i>	<i>CCI</i>
<i>R</i>	-0,414	-,680*
<i>G</i>	-0,416	-0,542
<i>B</i>	-0,276	-0,425
<i>H</i>	0,374	0,335
<i>S</i>	0,512	0,716**
<i>L</i>	-0,418	-0,601*
<i>L</i>	-0,410	-0,545
<i>a</i>	0,506	0,478
<i>b</i>	-0,394	-0,347
<i>H</i>	0,374	0,335
<i>S</i>	0,473	0,714**
<i>B</i>	-0,413	-0,540

* and ** indicate significant correlation at $P < 0.05$ and $P < 0.01$, respectively

Table VI shows Pearson's correlations of color coordinates with Chlorophyll Content Index (CCI) and Fractional Intercepted Photosynthetic Active Radiation (fIPAR).

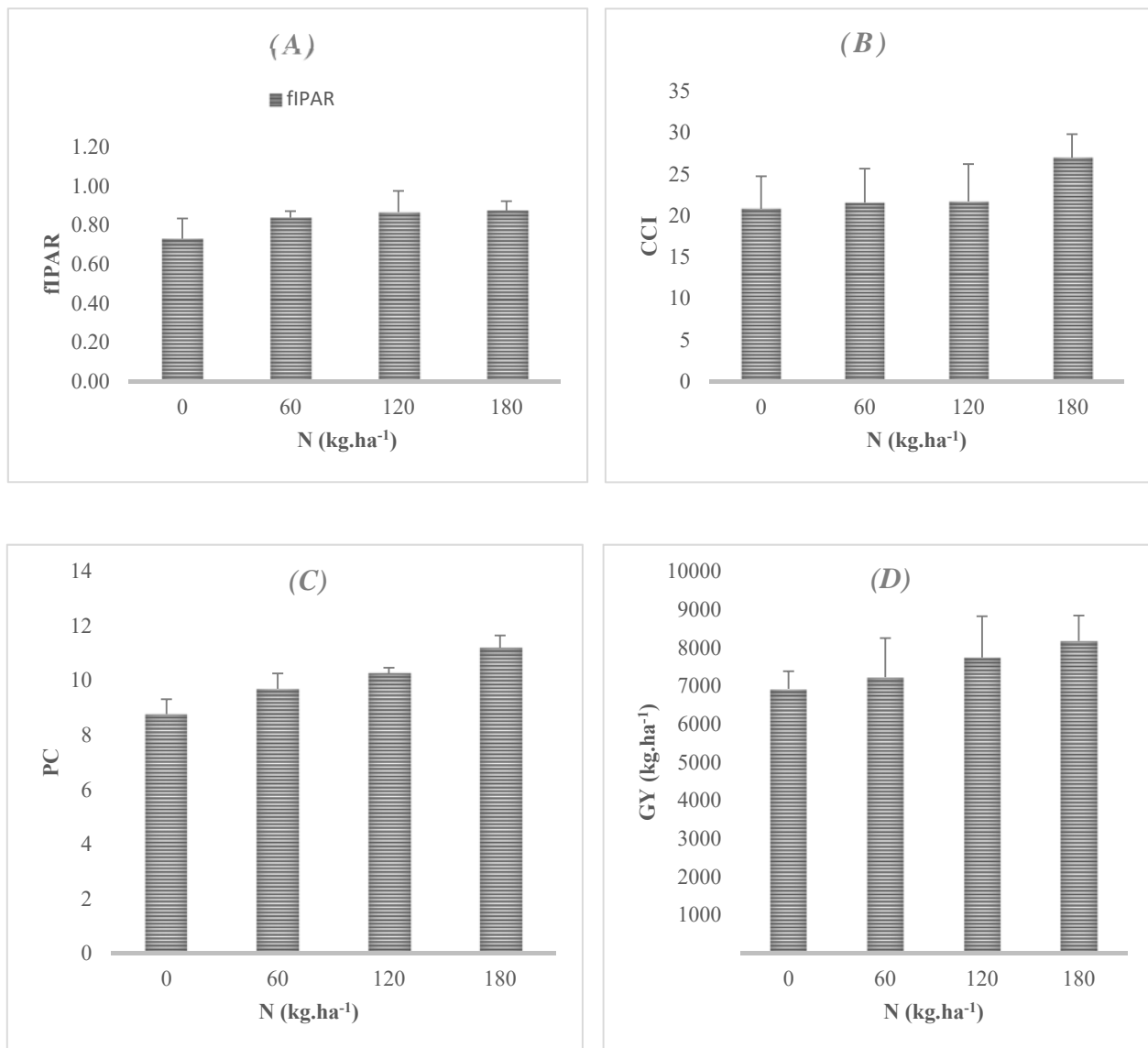
No correlation was recorded for fIPAR, hence the difficulty in determining barley biomass using color coordinates.

Among the color coordinates, only R (RGB), S (HSL), L (Lab), and S (HSB) which correlate with chlorophyll content; S (HSL) and S (HSB) show a positive correlation however R (RGB) and L (Lab) are negatively correlated with CCI.

The S (HSL) and S (HSB) indicate the saturation level and the L (Lab) and R (RGB) reflect the brightness. From one hand, for brightness, the two-color coordinates have a negative correlation, so the brighter the image the less chlorophyll there is. On the other hand, for saturation the correlation is positive; the higher the intensity of the color, the more chlorophyll is detected.

4.1.4. The capability of spectral indices at distinguishing crop N status and their effects on grain yield and protein content

Spectral indices are useful for estimating crop yield potential and basing in-season N fertilizer applications (Figure 5). For barley, the application of the four different treatments of N (0, 60, 120, and 180) didn't show any significant differences in spectral indices fIPAR, CCI, PC, BR, VARI, and GY. All the mentioned spectral indices didn't show significant variation ($P>0.05$) among N-treatments during the anthesis phenological stage.



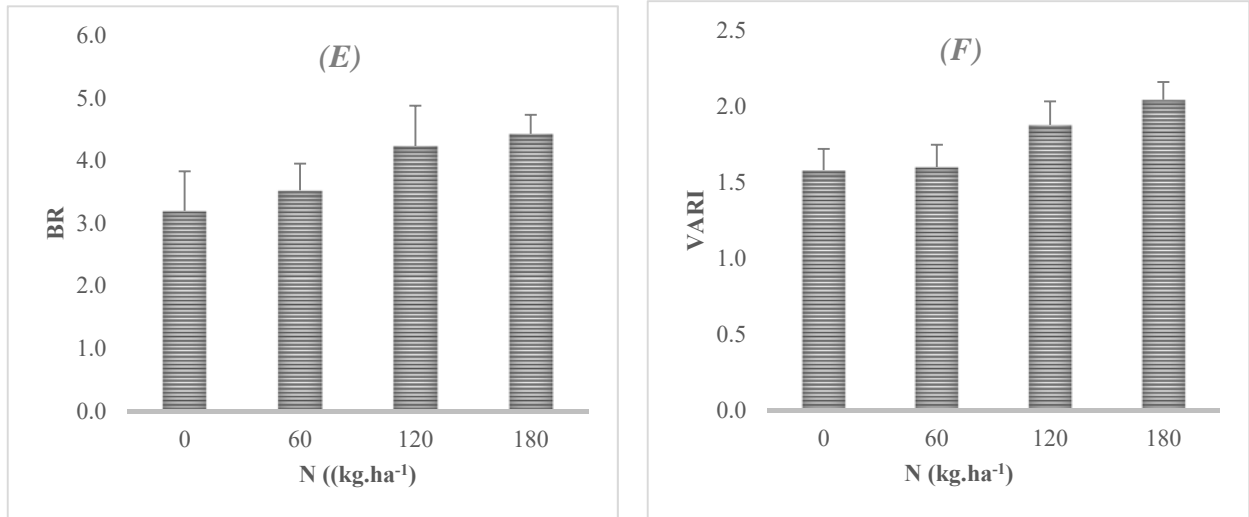


Figure 5: (A) Fractional Intercepted Photosynthetic Active Radiation (fIPAR), (B) leaf Chlorophyll Content Index (CCI), (C) Protein content (PC), (D) grain yield (GY), (E) Blue Red Simple Ratio (BR) and (F) Visible Atmosphericly Resistant Index (VARI) at anthesis phenological stage for barley. Data are average values for each treatment and bars represent the standard error of the mean ($n = 3$).

4.2. *Triticum aestivum* L

4.2. 1. *Optical indices (fIPAR and CCI) values*

Minor variations in fIPAR and CCI among N-treatments at the anthesis phenological stage were observed (Figure 6). Fractional Intercepted Photosynthetic Active Radiation (fIPAR) average values varies between $0,58 \pm 0,042$ to $0,67 \pm 0,042$ (average \pm Standard deviation) and CCI values range from $26,39 \pm 1,863$ to $34,27 \pm 1,863$ (average \pm Standard deviation. The differences between N treatments weren't significant for fIPAR ($P > 0,2$) and weakly significant for CCI ($P = 0,067$).

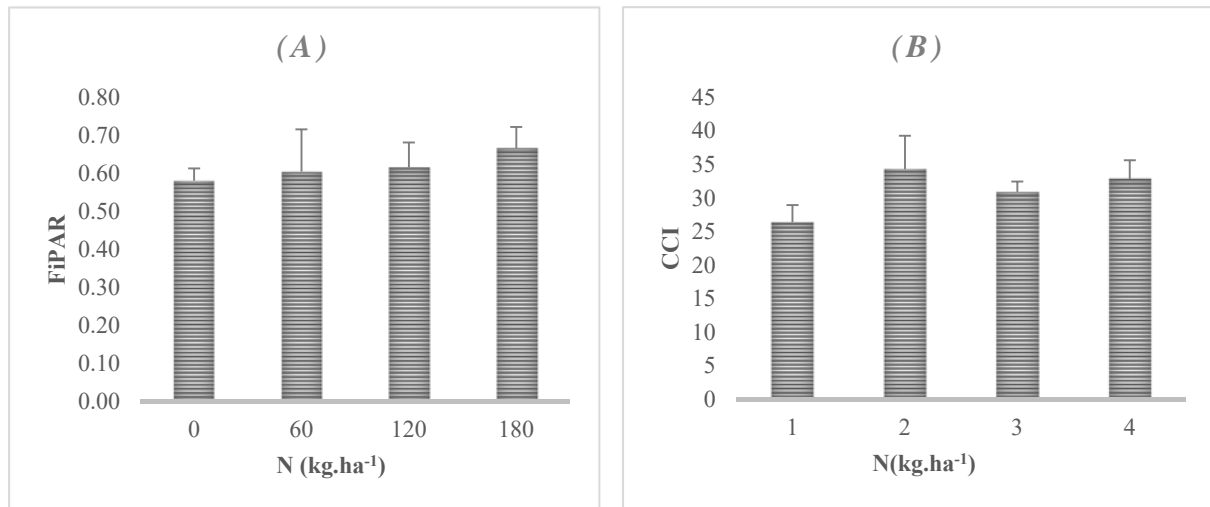


Figure 6 : (A) Fractional Intercepted Photosynthetic Active Radiation (fIPAR) and (B) leaf Chlorophyll Content Index (CCI) at the anthesis phenological stage for wheat. Data are average values for each treatment and bars represent the standard error of the mean ($n = 3$).

4.2. 2. *Relationships among crop data (biomass, and grain yield and grain protein content) and canopy biophysical attributes (fIPAR and CCI)*

The data obtained from fIPAR showed a highly significant correlation with all parameters, and the higher correlation was with biomass and yield parameters with 0,673 and 0,672 ($P < 0,01$) respectively (Table VII). On the other hand, the data obtained from the CCI showed a strong correlation with the PC with an average of 0,587 ($P < 0,01$).

Table VII: Correlation coefficients between the fraction of intercepted PAR (fIPAR), the chlorophyll content index (CCI), biomass yield, grain yield, and protein content for wheat at anthesis phenological stage (n = 12).

	Biomass avg (kg.ha ⁻¹)	Grain yield (GY) avg (kg.ha ⁻¹)	Protein content PC avg
FIPAR avg	,673*	,672*	,596*
CCI avg	,768**	,773**	,587*

* and ** indicate significant correlation at $P < 0,05$ and $P < 0,01$, respectively

4.2.3. Relationships between the fIPAR and CCI and spectral data (vegetation indices and color coordinates)

The vegetation indices derived from the combination of the visible (RGB) and infrared (NIR) bands have shown a significant correlation with the biophysical variables of the canopy fIPAR and CCI (Table VIII). The CCI and fIPAR correlation coefficients were almost of equal importance.

Among these indices, the NIR/R and NIR/G ratios with the NDVI and GNDVI index, respectively, outperformed the other indices when estimating the fIPAR, presenting a highly significant correlation $r = 0,818$; ($P < 0,01$).

For the CCI estimation, all calculated indices presented a highly significant correlation, the index that presented the highest correlation was the BR index with $r = 0,803$ ($P < 0,01$).

Table VIII: Correlation coefficients between the fraction of intercepted PAR (fIPAR), the chlorophyll content index (CCI), and the vegetation indexes (VI) obtained for wheat with a modified conventional digital camera (n = 12).

Bands	Relation	VI	fIPAR	CCI
NIR-VISIBLE	<i>NIR/R</i>	NDVI	,818**	,740**
		<i>SR</i>	,816**	,750**
	<i>NIR/G</i>	GNDVI	,818**	,727**
		<i>GSR</i>	,817**	,730**
	<i>B/R</i>	BR	,702*	,803**
	<i>G/R</i>	GR	,727**	,713**

VISIBLE		<i>NDVIg</i>	,725**	,705*
		<i>VARI</i>	,561	,800**
	<i>R/G/B</i>	<i>NDVIrgb</i>	,742**	,793**
		<i>SRrgb</i>		

* and ** indicate significant correlation at $P < 0,05$ and $P < 0,01$, respectively

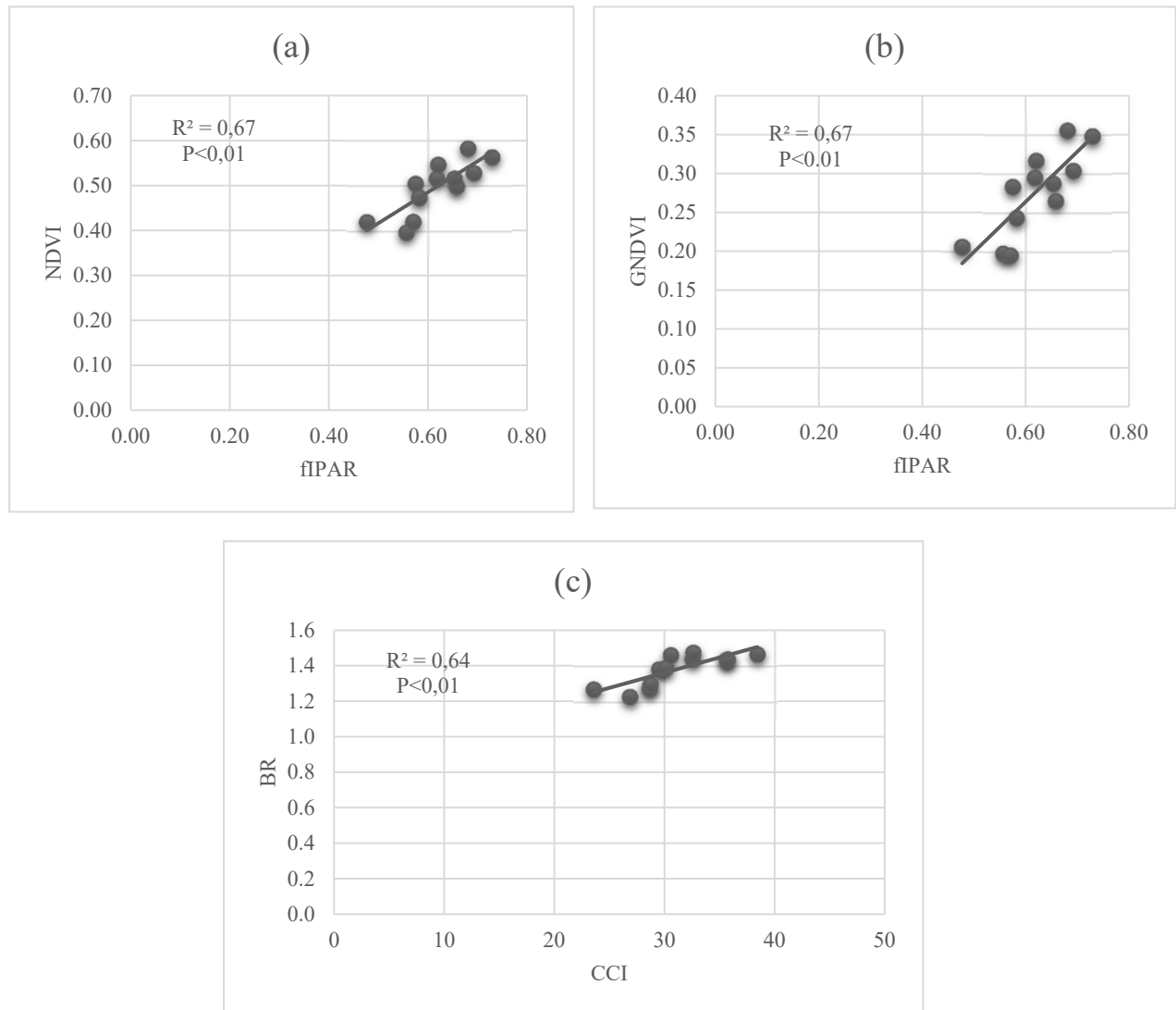


Figure 7: Correlations between the different vegetation indices of wheat and fIPAR and CCI: between the NDVI and GNDVI indices and fIPAR (a) and (b), and between VARI and CCI (c) ($n = 12$).

Table IX shows that all the indices showed a good correlation with GY and biomass with values varying between 0,696 and 0,789. On the other hand, only the BR, VARI, and NDVI_{rgb} indices correlate with GPC: 0,689 and 0,595 and 0,587 respectively ($P < 0,05$).

Table IX: Correlation coefficients between biomass, yield, and protein content and vegetation indices (VI) obtained for wheat with a modified conventional digital camera (n = 12).

	<i>VI</i>	<i>GY</i>	<i>Biomass</i>	<i>PC</i>
<i>NIR/R</i>	<i>NDVI</i>	,785**	,748**	0,518
	<i>SR</i>	,781**	,738**	0,499
<i>NIR/G</i>	<i>GNDVI</i>	,789**	,762**	0,536
	<i>GSR</i>	,777**	,746**	0,528
<i>B/R</i>	<i>BR</i>	,802**	,762**	,689*
<i>G/R</i>	<i>GR</i>	,696*	,627*	0,386
	<i>NDVI_g</i>	,688*	,620*	0,392
<i>R/G/B</i>	<i>VARI</i>	,794**	,741**	,595*
	<i>NDVI_{rgb}</i>	,783**	,728**	,587*
	<i>SR_{rgb}</i>			

* and ** indicate significant correlation at $P < 0,05$ and $P < 0,01$, respectively

Table X: The Pearson correlation values between the fIPAR and CCI and the parameters of different color coordinates of wheat.

	<i>fIPAR</i>	<i>CCI</i>
R	-,793**	-,723**
G	-,765**	-,686*
B	-,675*	-0,519
H	,667*	,665*
S	,578	,694*
L	-,661*	-,728**
L	-,637*	-,749**
a	,820**	,820**

b	-,787**	-,691*
H	,741**	,658*
S	,682	,744**
B	-,798**	-,709**

Pearson color coordinate correlations with Chlorophyll Content Index (CCI) and Fractional Intercepted Photosynthetic Active Radiation (fIPAR) are collated in Table X.

For fIPAR, all color coordinates except S (HSL) and S (HSB) correlate strongly with fIPAR; H (HSL), a (Lab), and H (HSB) are positively correlated with fIPAR while the rest have a negative correlation.

For CCI, strong correlations were recorded for all color coordinates except B (RGB); positive correlations were recorded for H (HSL), S (HSL), a (Lab), H (HSB), and S (HSB) coordinates, and other color coordinates were negatively correlated with chlorophyll content.

In both cases, L (HSL), L (Lab), and B (HSB), which are reflected at image brightness, are negatively correlated with CCI and fIPAR; The higher the brightness of the image, the lower the biomass and chlorophyll content.

For CCI, S (HSL) and S (HSB), a sign of saturation, showed a positive correlation; therefore the greater the intensity of the color, the more chlorophyll content is detected.

4.2. 4. The capability of spectral indices at distinguishing crop N status and their effects on grain yield and protein content.

The spectral indices including GY, GNDVI, and NDVI didn't present significant differences, while fIPAR, CCI, PC presented minor significant variations between the four N-treatment (Figure 8).

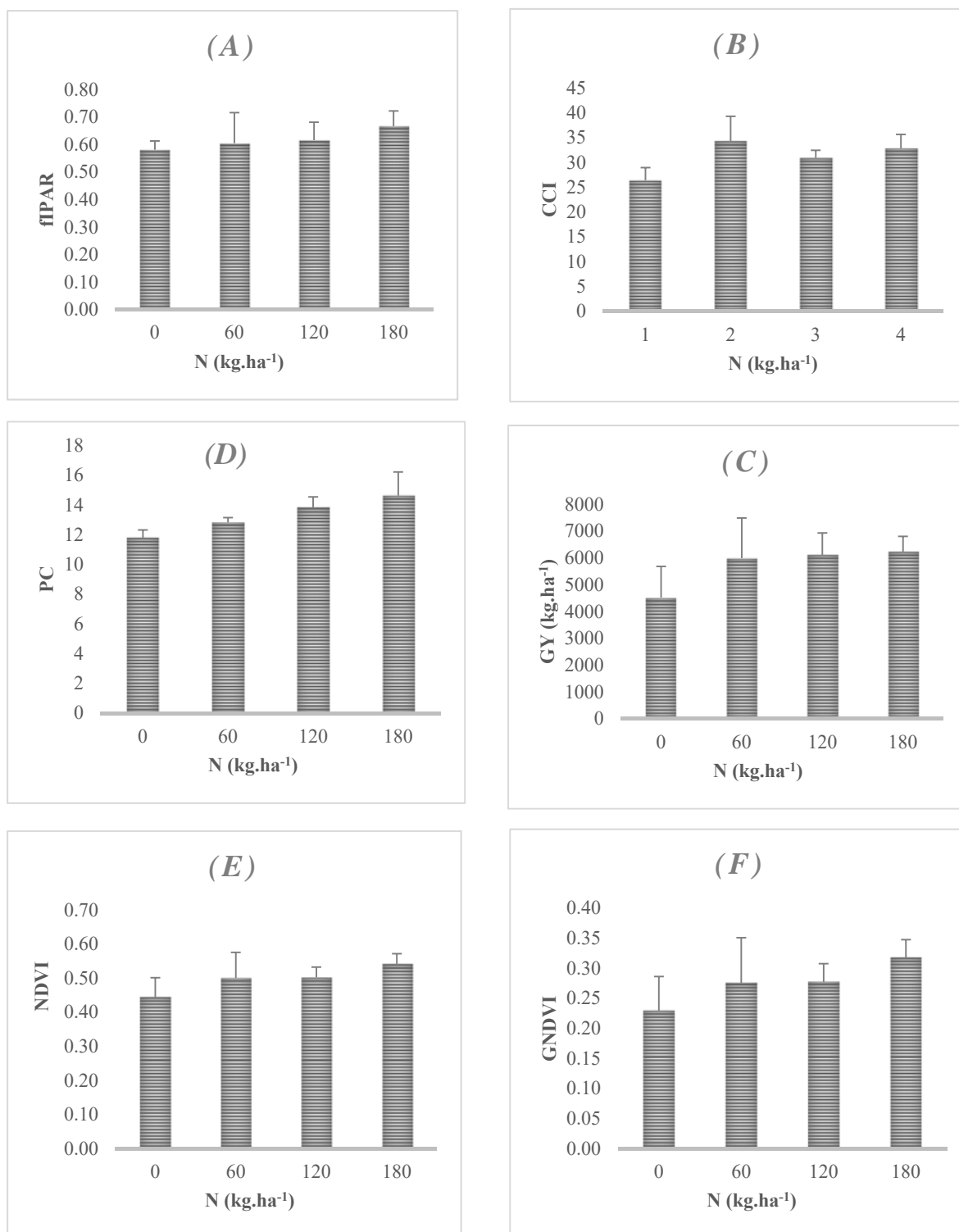


Figure 8 : (A) Fractional Intercepted Photosynthetic Active Radiation (fIPAR), (B) leaf Chlorophyll Content Index (CCI), (C) grain yield (GY), (D) Protein content (PC), (E) Normalized Difference Vegetation Index (NDVI) and (F) Green Normalized Vegetation Index (GNDVI) at anthesis phenological stage for wheat according to SNK. Data are average values for each treatment and bars represent the standard error of the mean (n = 3).

5. Discussion

The estimation of the nutrient content of plants is important in agricultural practices especially in enabling the application of precision farming. The overall aim of this study was mainly the estimation of N status and grain protein contents of *Hordeum vulgare* L and *Triticum aestivum* L from optical and spectral data extracted from a modified consumer-grade camera. Optical remote sensing methods were replaced by a conventional digital camera. The capability of these optical and spectral data to detect differences in crop N status and their influences on grain yield and protein content was compared.

Many recent studies have investigated the use of digital cameras to characterize crop growth and nutrient status. Multiple have already analyzed the potentiality of vegetation indices derived from modified conventional cameras (RGB) in the estimation of chlorophyll and nitrogenous status for wheat and barley (Fernández et al., 2019; Jiang et al., 2019).

In the current study, the BR vegetation index showed a strong correlation with fIPAR for barley while, for wheat, all NIR and VISIBLE indices were highly correlated with fIPAR, with; NDVI and GNDVI among the most significant. These results are similar to those reported by other studies in which the combination of both NIR bands and red bands are the most optimal for adequately characterize fIPAR (Kyratzis et al., 2017; Liebisch et al., 2015; Quemada et al., 2014).

For CCI, all vegetation indices studied were highly correlated with CCI especially VARI and BR bands for both wheat and barley. Besides, vegetation indices derived from the combination of visible (RGB) and near-infrared (NIR) bands showed a significant correlation with canopy biophysical variables: fIPAR and CCI. These correlations were higher for CCI than for fIPAR in barley, and the opposite in wheat.

According to Fernández et al.2019 who carried out a study on wheat, the big differences in CCI between non-fertilized and fertilized treatments were observed at the anthesis stage. Moreover, the correlations between vegetation indices and canopy biophysical variables (fIPAR and CCI) were higher with fIPAR than for CCI at anthesis, which is similar to this study's results in the wheat section and dissimilar with the barley section.

In agreement with previous studies in wheat (Fernández et al., 2019; Filella et al., 1995), the blue to the red ratio (BR) was found to be significantly related to chlorophyll content. Contrastingly, Schirrmann et al. (Schirrmann et al., 2016) did not find a significant correlation between BR and tissue total N content whereas BR captured variation in biomass and LAI.

In addition to the chlorophyll content and fIPAR estimation, all ratios and several indices presented highly significant correlations with biomass and grain yield especially BR and VARI for both wheat and barley. For protein content, only VARI and BR successfully showed significant correlations in the barley case, whereas BR, VARI, and NDVI_{rgb} had a good capacity to estimate the grain protein content in wheat. Other results found by Kyratzis et al (2017) and Quemada et al. (2014) showed that the GNDVI index has a good capacity to estimate wheat aerial biomass and grain yield. RGB indices in this study showed comparable capability at assessing biomass and yield than NIR band based indices, while they presented dissimilar abilities to estimate CCI and fIPAR depending on the species. That might be related to the timing of image acquisition; Differences in crop status at the timing of image acquisition related to growth (soil cover and LAI), phenology (canopy greenness) as well as to the incidence of other stresses, particularly water stress, might mask the crop spectral response to N status (Gabriel et al., 2017).

(Yamori et al., 2016) reported that leaf photosynthesis was the most significant factor for biomass and grain yield. In contrast, few studies have focused on the relationship between the photosynthetic capacity of crops and biochemical photosynthetic components such as leaf chlorophyll or carotenoid content to develop a biomass or yield model (Houborg et al., 2013). Chlorophyll is an important part of the Calvin–Benson cycle, and it is responsible for harvesting light during photosynthesis, which results in the excitation of electrons that are used to drive the production of nicotinamide adenine dinucleotide phosphate and chemical energy in the form of adenosine triphosphate (Palareti et al., 2016). It also indicates nutritional status as a result of N fertilizer, which serves as a reliable means to estimate the function of N fertilizer (Amalero et al., 2003).

This study pointed out also the good correlation of CCI and fIPAR with biomass, and grain yield, and grain protein content in wheat treatments; CCI was highly correlated with biomass, grain yield, and grain protein content than fIPAR. For barley, fIPAR only permits the estimation

of Grain yield, and CCI is highly correlated to biomass and grain yield. Whereas grain protein content correlates with none of the two canopy biophysical variables.

All calculated indices presented significant corrections in the estimation of the biomass and grain yield and just BR, VARI and NDVI_{rgb} correlate with grain protein content.

While using a modified consumer-grade camera, the modification of filters (IR) while taking images might be another factor that affects the information obtained through the cameras. The modification of the camera made by removing the IR filter negatively influences the operating capacity of the three RGB channels. This is since the energy captured by the CMOS sensor is less than in the unmodified camera, so that the exposure times are longer, leading to the acquisition of data becoming susceptible to interference by vibration frequencies (Lebourgeois et al., 2008; Mishra et al., 2016).

N requirements as already mentioned can be estimated from chlorophyll concentration and remote sensing of crop N status is feasible in the visible spectral bands due to the close association between N and chlorophyll content. Anterior studies have explored the capability of vegetation indices derived from commercial-grade cameras (RGB) at estimating either N or chlorophyll content. In wheat, indices based on green and red bands have been related to N content (Fernández et al., 2019; Yousfi et al., 2016). Similarly, in this study, ratio and normalized difference indices based on green, blue, and red bands (i.e., GR, VARI, NDVI_{rgb}) were found to be closely related to chlorophyll content. This study suggests other indices in chlorophyll estimation including NDVI, SR, and NDVI_g; these three indices could be used, in addition to others, to estimate chlorophyll content.

The results obtained in this study pointed out that vegetation indices based on modified conventional cameras can have great potential at assessing the N status of the crop. It highlighted the possible successful use of several and multiple vegetation indices to detect biophysical and agronomic parameters, indifference with what (Agapiou et al., 2012) reported where more than one vegetation index can be used successfully to attend and monitor N status.

6. CONCLUSIONS AND FUTURE LINES

The vegetation indices derived from a modified conventional camera provided reliable estimates in the measurements of the different parameters (fIPAR, CCI, GYP, biomass, and grain yield) of the studied crops *Hordeum vulgare* L. and *Triticum aestivum* L.

RGB-NIR based indices derived from a modified conventional camera were able to capture variation in fIPAR and chlorophyll content especially NDVI and GNDVI. Furthermore, RGB indices, particularly BR and VARI, provided also chlorophyll content and fIPAR estimates.

To conclude, the results obtained in this study highlighted the potential of standard and modified consumer grade cameras as simple, affordable, fast, and low-cost tools for N status assessment as for the prediction of chlorophyll content, fIPAR, biomass, and grain yield protein.

This study and the presented analyses could inspire future works, including :

- ✓ The use of the aerial vehicle could be implemented to obtain ultra-high resolution areas with higher spatial resolution.
- ✓ The development of low-cost remote sensing techniques to determine N nutrient could be a valuable tool to improve the management of fertilization, increase the efficiency of its use, and reduce the environmental impacts associated with its misuse.

LIST OF REFERENCES

- Agapiou, A., Hadjimitsis, D. G., & Alexakis, D. D. (2012). Evaluation of broadband and narrowband vegetation indices for the identification of archaeological crop marks. *Remote Sensing*, 4(12), 3892–3919. <https://doi.org/10.3390/rs4123892>
- Amalero, E. G., Ingua, G. L., Erta, G. B., & Emanceau, P. L. (2003). Review article Methods for studying root colonization by introduced. *Agronomie*, 23, 407–418. <https://doi.org/10.1051/agro>
- Berger, K., Verrelst, J., Féret, J. B., Wang, Z., Woche, M., Strathmann, M., Danner, M., Mauser, W., & Hank, T. (2020). Crop nitrogen monitoring: Recent progress and principal developments in the context of imaging spectroscopy missions. *Remote Sensing of Environment*, 242(December 2019). <https://doi.org/10.1016/j.rse.2020.111758>
- Cabrera-Bosquet, L., Molero, G., Stellacci, A., Bort, J., Nogués, S., & Araus, J. (2011). NDVI as a potential tool for predicting biomass, plant nitrogen content and growth in wheat genotypes subjected to different water and nitrogen conditions. *Cereal Research Communications*, 39(1), 147–159. <https://doi.org/10.1556/CRC.39.2011.1.15>
- Cárdenas-Navarro, R., Sánchez-Yáñez, J. M., Farías-Rodríguez, R., & Peña-Cabriales, J. J. (2004). Los Aportes De Nitrógeno En La Agricultura. *Revista Chapingo Serie Horticultura*, X(2), 173–178. <https://doi.org/10.5154/r.rchsh.2002.07.039>
- Chen, D., & Brutsaert, W. (1998). Satellite-sensed distribution and spatial patterns of vegetation parameters over a tallgrass prairie. *Journal of the Atmospheric Sciences*, 55(7), 1225–1238. [https://doi.org/10.1175/1520-0469\(1998\)055<1225:SSDASP>2.0.CO;2](https://doi.org/10.1175/1520-0469(1998)055<1225:SSDASP>2.0.CO;2)
- Corwin, D. L., Lesch, S. M., Shouse, P. J., Sopper, R., & Ayars, J. E. (2004). *Characterizing Soil Spatial Variability for Precision Agriculture Using Geophysical Measurements*. March 2015, 26–38. <https://doi.org/10.4133/1.2923341>
- Efretuei, A., Gooding, M., White, E., Spink, J., & Hackett, R. (2016). Effect of nitrogen fertilizer application timing on nitrogen use efficiency and grain yield of winter wheat in Ireland. *Irish Journal of Agricultural and Food Research*, 55(1), 63–73. <https://doi.org/10.1515/ijafr-2016-0006>
- Fernández, E., Gorchs, G., & Serrano, L. (2019). Use of consumer-grade cameras to assess wheat N status and grain yield. *PLoS ONE*, 14(2), 1–18. <https://doi.org/10.1371/journal.pone.0211889>

- Filella, I., Serrano, L., Serra, J., & Penuelas, J. (1995). Evaluating wheat nitrogen status with canopy reflectance indices and discriminant analysis. *Crop Science*, 35(5), 1400–1405. <https://doi.org/10.2135/cropsci1995.0011183X003500050023x>
- Fischbeck, G., & Muller, R. (1990). *und Verteilung der mineralischen N-Düngung*. 311, 297–311.
- Gabriel, J. L., Zarco-Tejada, P. J., López-Herrera, P. J., Pérez-Martín, E., Alonso-Ayuso, M., & Quemada, M. (2017). Airborne and ground level sensors for monitoring nitrogen status in a maize crop. *Biosystems Engineering*, 160, 124–133. <https://doi.org/10.1016/j.biosystemseng.2017.06.003>
- Gauer, L. E., Grant, C. A., Bailey, L. D., & Gehl, D. T. (1992). Effects of nitrogen fertilization on grain protein content, nitrogen uptake, and nitrogen use efficiency of six spring wheat (*Triticum aestivum* L.) cultivars, in relation to estimated moisture supply. *Canadian Journal of Plant Science*, 72(1), 235–241. <https://doi.org/10.4141/cjps92-026>
- Houborg, R., Cescatti, A., Migliavacca, M., & Kustas, W. P. (2013). Satellite retrievals of leaf chlorophyll and photosynthetic capacity for improved modeling of GPP. *Agricultural and Forest Meteorology*, 117(1), 10–23. <https://doi.org/10.1016/j.agrformet.2013.04.006>
- Jay, S., Maupas, F., Bendoula, R., & Gorretta, N. (2017). Retrieving LAI, chlorophyll and nitrogen contents in sugar beet crops from multi-angular optical remote sensing: Comparison of vegetation indices and PROSAIL inversion for field phenotyping. *Field Crops Research*, 210(September), 33–46. <https://doi.org/10.1016/j.fcr.2017.05.005>
- Jiang, J., Cai, W., Zheng, H., Cheng, T., Tian, Y., Zhu, Y., Ehsani, R., Hu, Y., Niu, Q., Gui, L., & Yao, X. (2019). Using digital cameras on an unmanned aerial vehicle to derive optimum color vegetation indices for leaf nitrogen concentration monitoring in winter wheat. *Remote Sensing*, 11(22). <https://doi.org/10.3390/rs11222667>
- Kyratzis, A. C., Skarlatos, D. P., Menexes, G. C., Vamvakousis, V. F., & Katsiotis, A. (2017). Assessment of vegetation indices derived by UAV imagery for durum wheat phenotyping under a water limited and heat stressed Mediterranean environment. *Frontiers in Plant Science*, 8(June), 1–14. <https://doi.org/10.3389/fpls.2017.01114>
- Lebourgeois, V., Bégué, A., Labbé, S., Mallavan, B., Prévot, L., & Roux, B. (2008). Can commercial digital cameras be used as multispectral sensors? A crop monitoring test. *Sensors*, 8(11), 7300–7322. <https://doi.org/10.3390/s8117300>
- Li, F., Gnyp, M. L., Jia, L., Miao, Y., Yu, Z., Koppe, W., Bareth, G., Chen, X., & Zhang, F. (2008). Estimating N status of winter wheat using a handheld spectrometer in the North China Plain. *Field Crops Research*, 106(1), 77–85.

<https://doi.org/10.1016/j.fcr.2007.11.001>

- Liang, L., Schwartz, M. D., & Fei, S. (2011). Validating satellite phenology through intensive ground observation and landscape scaling in a mixed seasonal forest. *Remote Sensing of Environment*, *115*(1), 143–157. <https://doi.org/10.1016/j.rse.2010.08.013>
- Liebisch, F., Kirchgessner, N., Schneider, D., Walter, A., & Hund, A. (2015). Remote, aerial phenotyping of maize traits with a mobile multi-sensor approach. *Plant Methods*, *11*(1). <https://doi.org/10.1186/s13007-015-0048-8>
- Ma, G., Liu, W., Li, S., Zhang, P., Wang, C., Lu, H., Wang, L., Xie, Y., Ma, D., & Kang, G. (2019). Determining the optimal N input to improve grain yield and quality in winter wheat with reduced apparent N loss in the north China plain. *Frontiers in Plant Science*, *10*(February), 1–12. <https://doi.org/10.3389/fpls.2019.00181>
- Mantai, R. D., Silva, J. A. G. da, Arenhardt, E. G., Sausen, A. T. Z. R., Binello, M. O., Bianchi, V., Silva, D. R. da, & Bandeira, L. M. (2016). The Dynamics of Relation Oat Panicle with Grain Yield by Nitrogen. *American Journal of Plant Sciences*, *07*(01), 17–27. <https://doi.org/10.4236/ajps.2016.71003>
- Mishra, P. K., Pandey, S., & Biswash, S. K. (2016). Efficient Resource Management by Exploiting D2D Communication for 5G Networks. *IEEE Access*, *4*, 9910–9922. <https://doi.org/10.1109/ACCESS.2016.2602843>
- Mulla, D. J. (2013). Twenty five years of remote sensing in precision agriculture: Key advances and remaining knowledge gaps. *Biosystems Engineering*, *114*(4), 358–371. <https://doi.org/10.1016/j.biosystemseng.2012.08.009>
- Nakano, H., Morita, S., & Kusuda, O. (2008). Effect of nitrogen application rate and timing on grain yield and protein content of the bread wheat cultivar “Minaminokaori” in southwestern Japan. *Plant Production Science*, *11*(1), 151–157. <https://doi.org/10.1626/pps.11.151>
- Nijland, W., de Jong, R., de Jong, S. M., Wulder, M. A., Bater, C. W., & Coops, N. C. (2014). Monitoring plant condition and phenology using infrared sensitive consumer grade digital cameras. *Agricultural and Forest Meteorology*, *184*, 98–106. <https://doi.org/10.1016/j.agrformet.2013.09.007>
- Palareti, G., Legnani, C., Cosmi, B., Antonucci, E., Erba, N., Poli, D., Testa, S., & Tosetto, A. (2016). Comparison between different D-Dimer cutoff values to assess the individual risk of recurrent venous thromboembolism: Analysis of results obtained in the DULCIS study. *International Journal of Laboratory Hematology*, *38*(1), 42–49. <https://doi.org/10.1111/ijlh.12426>

- Putra, B. T. W., Soni, P., Marhaenanto, B., Pujiyanto, Sisbudi Harsono, S., & Fountas, S. (2020). Using information from images for plantation monitoring: A review of solutions for smallholders. *Information Processing in Agriculture*, 7(1), 109–119. <https://doi.org/10.1016/j.inpa.2019.04.005>
- Quemada, M., Gabriel, J. L., & Zarco-Tejada, P. (2014). Airborne hyperspectral images and ground-level optical sensors as assessment tools for maize nitrogen fertilization. *Remote Sensing*, 6(4), 2940–2962. <https://doi.org/10.3390/rs6042940>
- Richardson, A. D., Duigan, S. P., & Berlyn, G. P. (2002). An evaluation of noninvasive methods to estimate foliar chlorophyll content. *New Phytologist*, 153(1), 185–194. <https://doi.org/10.1046/j.0028-646X.2001.00289.x>
- Scharf, P., & Grundler, J. (n.d.). *re ch te iv ns e v io e n . rs m io is n so -- ur Se i . e e du in Missouri PRACTICES for in collaboration with.*
- Schirrmann, M., Giebel, A., Gleiniger, F., Pflanz, M., Lentschke, J., & Dammer, K. H. (2016). Monitoring agronomic parameters of winter wheat crops with low-cost UAV imagery. *Remote Sensing*, 8(9). <https://doi.org/10.3390/rs8090706>
- Soudani, K., Hmimina, G., Delpierre, N., Pontailier, J. Y., Aubinet, M., Bonal, D., Caquet, B., de Grandcourt, A., Burban, B., Flechard, C., Guyon, D., Granier, A., Gross, P., Heinesh, B., Longdoz, B., Loustau, D., Moureaux, C., Ourcival, J. M., Rambal, S., ... Dufrêne, E. (2012). Ground-based Network of NDVI measurements for tracking temporal dynamics of canopy structure and vegetation phenology in different biomes. *Remote Sensing of Environment*, 123, 234–245. <https://doi.org/10.1016/j.rse.2012.03.012>
- Tsouros, D. C., Bibi, S., & Sarigiannidis, P. G. (2019). A review on UAV-based applications for precision agriculture. *Information (Switzerland)*, 10(11). <https://doi.org/10.3390/info10110349>
- Vasanthan, T., & Hoover, R. (2009). Barley Starch: Production, Properties, Modification and Uses. In *Starch* (Third Edit). Elsevier Inc. <https://doi.org/10.1016/B978-0-12-746275-2.00016-1>
- Vian, A. L., Bredemeier, C., Turra, M. A., Giordano, C. P. da S., Fochesatto, E., da Silva, J. A., & Drum, M. A. (2018). Nitrogen management in wheat based on the normalized difference vegetation index (NDVI). *Ciencia Rural*, 48(9), 1–9. <https://doi.org/10.1590/0103-8478cr20170743>
- Vitousek, P. M., Naylor, R., Crews, T., David, M. B., Drinkwater, L. E., Holland, E., Johnes, P. J., Katzenberger, J., Martinelli, L. A., Matson, P. A., Nziguheba, G., Ojima, D., Palm, C. A., Robertson, G. P., Sanchez, P. A., Townsend, A. R., & Zhang, F. S. (2009).

- Nutrient imbalances in agricultural development. *Science*, 324(5934), 1519–1520.
<https://doi.org/10.1126/science.1170261>
- Weiss, M., Jacob, F., & Duveiller, G. (2020). Remote sensing for agricultural applications: A meta-review. *Remote Sensing of Environment*, 236(November 2019), 111402.
<https://doi.org/10.1016/j.rse.2019.111402>
- Wilkinson, L. G. (2019). *Molecular and genetic cues influencing ovule development in barley (Hordeum vulgare)*. February.
- Xie, Q., Dash, J., Huang, W., Peng, D., Qin, Q., Mortimer, H., Casa, R., Pignatti, S., Laneve, G., Pascucci, S., Dong, Y., & Ye, H. (2018). Vegetation Indices Combining the Red and Red-Edge Spectral Information for Leaf Area Index Retrieval. *IEEE Journal of Selected Topics in Applied Earth Observations and Remote Sensing*, 11(5), 1482–1492.
<https://doi.org/10.1109/JSTARS.2018.2813281>
- Yamori, W., Kondo, E., Sugiura, D., Terashima, I., Suzuki, Y., & Makino, A. (2016). Enhanced leaf photosynthesis as a target to increase grain yield: Insights from transgenic rice lines with variable Rieske FeS protein content in the cytochrome b6/f complex. *Plant Cell and Environment*, 39(1), 80–87. <https://doi.org/10.1111/pce.12594>
- Yang, C., Westbrook, J. K., Suh, C. P. C., Martin, D. E., Hoffmann, W. C., Lan, Y., Fritz, B. K., & Goolsby, J. A. (2014). An airborne multispectral imaging system based on two consumer-grade cameras for agricultural remote sensing. *Remote Sensing*, 6(6), 5257–5278. <https://doi.org/10.3390/rs6065257>
- Yousfi, S., Kellas, N., Saidi, L., Benlakehal, Z., Chaou, L., Siad, D., Herda, F., Karrou, M., Vergara, O., Gracia, A., Araus, J. L., & Serret, M. D. (2016). Comparative performance of remote sensing methods in assessing wheat performance under Mediterranean conditions. *Agricultural Water Management*, 164, 137–147.
<https://doi.org/10.1016/j.agwat.2015.09.016>